NANO LETTERS

2003
Vol. 3, No. 4
479−483

Field Effect Transistor Based on a Modified DNA Base

Giuseppe Maruccio,*,† Paolo Visconti, Valentina Arima, Stefano D'Amico, Adriana Biasco, Eliana D'Amone, Roberto Cingolani, and Ross Rinaldi

National Nanotechnology Laboratory of INFM, University of Lecce, Via per Arnesano, 73100 Lecce, Italy

Stefano Masiero, Tatiana Giorgi, and Giovanni Gottarelli

Department of Organic Chemistry, University of Bologna, 40126 Bologna, Italy

Received January 24, 2003; Revised Manuscript Received February 11, 2003

ABSTRACT

In this work, a field effect transistor based on a deoxyguanosine derivative (a DNA base) is demonstrated. Our experiments on transport through the source and drain electrodes interconnected by self-assembled guanine ribbons (Gottarelli et al. *Helv. Chim. Acta* 1998, *81*, 2078; Gottarelli et al. *Chem. Eur. J.* 2000, *6*, 3242; Giorgi et al. *Chem Eur. J.* 2002, *8*, 2143) suggest that these devices behave like p-channel MOSFETs. The devices exhibit a maximum voltage gain of 0.76. This prototype transistor represents a starting point toward the development of biomolecular electronic devices.

Modern electronics has to face the restrictions dictated by the laws of physics when the minimum feature size of a chip is reduced below a certain length (typically thought to be less than approximately 100 nm). Molecular electronics is proposed as an alternative approach to Si nanoelectronics to build integrated devices. Though this needs a cross-disciplinary effort (such as merging chemical, biological, and physical expertise), the molecular approach has the interesting advantage of high reproducibility, due to the self-organization and recognition properties[1,2] of the building blocks (the molecules), and the possibility of implementation of novel functional devices[3−5] exploiting unusual mechanisms, such as charge transfer, $\pi-\pi$ stack conductivity, molecular rectification,[6,7] etc. In addition, organic materials require relatively easy and cheap processing technologies for large area and large scale integration, such as spin-coating and inprint methods.

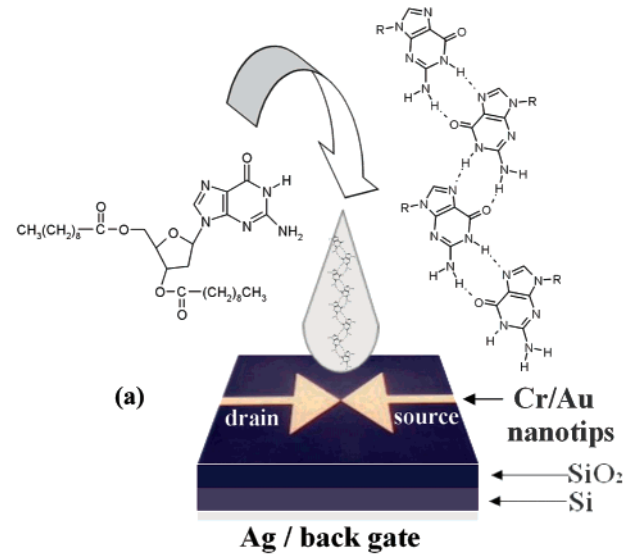
Recently, key demonstrations of molecular electronic devices have been reported, primarily through the use of carbon nanotubes[8,9] and polymers,[10] suggesting that the obstacles to the accomplishment of molecular electronic devices are more technical than conceptual. In particular, the demonstration of a three-terminal field effect device (field effect transistor) consisting of source (s) and drain (d) contacts interconnected by a molecular layer, and a third contact (gate) to modulate the drain−source current (I_{ds}), is a crucial step for the development of a molecular electronics road map. Nevertheless, most of the devices obtained so far have used disordered molecular layers (obtained by evaporation or spin-coating) or single molecules with tremendous interconnection problems. An alternative route is to exploit conduction of self-assembled biomolecules to achieve devices based on engineered highly ordered layers (bottom-up approach), taking advantage of the specific reactivity of molecules having functional groups with affinity for specific surfaces and/or molecules. Advances in the synthesis of biomolecules and in nanofabrication techniques enable the fabrication of such devices, thus permitting to verify whether molecular electronics may out perform Moore's law for circuit integration, beyond the limits of Si technology.

Our nanodevices were fabricated starting from a deoxyguanosine derivative ($dG(C_{10})_2$), whose assembled molecular structure is shown in Figure 1a. Guanosine has been chosen because of its peculiar sequence of H-bond donor or acceptor groups, and because it has the lowest oxidation potential among the DNA bases, which favors self-assembly and carrier transport, respectively. Previous work[1] demonstrates the arrangement of these molecules in ordered, periodic structures (on a length scale of about 100 nm) and the correlation between supramolecular ordering and conduction properties,[11] by means of combined AFM and transport studies. Such a guanosine supramolecular assembly has the form of long ribbons (see Figure 1a), with a strong intrinsic dipole moment[11] along the ribbon axis which causes current rectification in transport experiments.[12] Single-crystal X-ray

* To whom correspondence should be addressed. E-mail: giuseppe.maruccio@unile.it.

† Also with the Department of Physics, University of Lecce.

10.1021/nl034046c CCC: $25.00 © 2003 American Chemical Society
Published on Web 03/20/2003



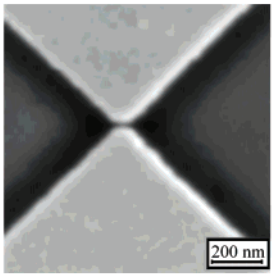


Figure 1. Self-organized ribbon of $dG(C_{10})_2$ and the nanodevice structure used in this study. (a) Self-assembly and cast deposition of $dG(C_{10})_2$ on the three-terminal device, consisting of two arrow-shaped Cr/Au (6 nm/35 nm thick) electrodes on a SiO_2 substrate and a third Ag back electrode (not to scale). Samples were obtained by depositing a 2 μL drop of a 3.5×10^{-4} M solution of $dG(C_{10})_2$ in chloroform. All devices were systematically tested before the deposition of drops and no significant current was observed. (b) High magnification SEM image of two Cr/Au nanotips with separation of 20 nm.

diffraction data[1c] for an analogous guanosine derivative show that, in the solid state, the ribbons are parallel: their dipoles are parallel and the crystal displays second harmonic generation.

The prototype structure investigated here is a planar metal−insulator−metal nanojunction, consisting of two arrow-shaped metallic electrodes facing each other and connected by the supramolecular structures. Such a configuration allows us to perform in-plane transport experiments across the molecular ribbons. A third electrode (gate) is deposited on the back of the device to produce a field effect transistor (see Figure 1a). Electron beam lithography (LV1 Lion Leica system) followed by a lift-off process has been used to fabricate the three-terminal nanodevices. These consist of two Cr/Au (6 nm/35 nm) electrodes on Si/SiO_2 substrate (see Figure 1b) and an Ag control electrode on the back of the Si substrate. Source−drain separation in the range 20−100 nm were reproducibly obtained.[13] All devices were inspected by plane-view scanning electron microscopy

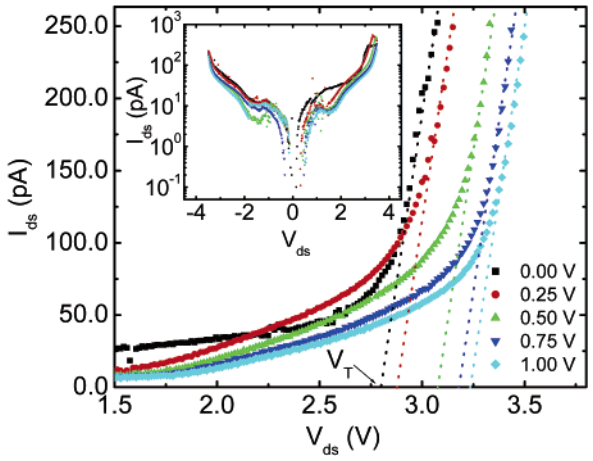


Figure 2. Characteristics of the three-terminal deoxyguanosine device with an electrode separation of 40 nm. Dependence of the drain−source current (I_{ds}) on the voltage (V_{ds}) at discrete gate voltages (V_G). The voltage threshold (V_T), indicating the onset of conduction, can be modulated by tuning the control gate voltage V_G. The dashed lines extrapolate V_T for any V_G value. (Inset) Log plot of the full current−voltage curves at different V_G.

(SEM) in order to check for the occurrence of defects and to measure the separation between the Cr/Au nanotips.

The hybrid nanodevices were fabricated by room-temperature cast deposition. Transport experiments were performed by changing the gate voltage (V_G) in order to investigate its influence on the current (I_{ds}) between the source (s) and drain (d) electrodes, and to evaluate the response of the nanodevices upon variation of V_G (see Figure 1). Current−voltage experiments were carried out by using a semiconductor parameter analyzer (HP Agilent 4155B) in the voltage range between −3.5 and 3.5 V, at room temperature and ambient pressure. Before the deposition of molecules, all devices were tested to verify that the channel was insulated (resistance as large as 100 GΩ up to 3.5 V).

Typical $I-V$ curves under forward bias at different gate bias are reported in Figure 2. The entire current−voltage characteristics on log scale are displayed in the inset of Figure 2. They are asymmetric, with a rectification ratio (RR), defined at a fixed drain−source voltage V_{ds} as

$$\mathrm{RR}(V) = I(V)/I(-V) \approx 3$$

This is the typical value obtained in most samples,[12] suggesting that the intrinsic dipole moment is partially preserved in the supramolecular layer connecting the electrodes, and induces an asymmetry in the charge pathway, resulting in a preferential direction for the current flow. We have also simultaneously measured the current between the planar electrodes and the back gate, finding values as low as a few pA and a negligible variation with V_G, demonstrating the good insulation of the back electrode. We mainly measure the conductance of the substrate when V_{ds} is lower than 1.5 V. In the range between 1.5 and 3.5 V the current−voltage characteristics are almost linear with resistances of tens of GΩ, indicating that this system behaves like an insulator at low voltages. The current rises steeply above a threshold

voltage (V_T) of the order of 3 V following an exponential dependence. The extent of the low-conductivity region observed in the voltage range between −3 V and 3 V increases with increasing V_G. V_T can be extrapolated by fitting the different $I-V$ characteristics for each gate voltage, by means of a straight line of constant resistance (dotted lines in Figure 2). Figure 3 (right-hand scale) displays the threshold voltage (V_T) as a function of the gate voltage, showing a linear dependence on V_G.

The current at fixed drain-source voltage decreases with V_G (Figure 3a, left-hand scale) as in a p-channel MOSFET. Using the small signal equivalent circuit for a MOS transistor, shown in Figure 3b, we can evaluate the parameters of our device. This device can be depicted by means of a current source (depending on V_G) and a resistance. The transconductance g_m is defined as

$$g_m = \left.\frac{\partial I_{ds}}{\partial V_G}\right|_{V_{ds}=\text{const}}$$

where g_m quantifies the dependence of the drain−source current I_{ds} on the gate voltage V_G at fixed drain−source voltage. The output resistance r_o takes into account the effect of the drain−source current, I_{ds}, modulation by the drain−source voltage, V_{ds}, when the gate−source voltage V_G is kept constant, and is defined as

$$r_o = \left.\left(\frac{\partial I_{ds}}{\partial V_{ds}}\right)^{-1}\right|_{V_G=\text{const}}$$

We have extracted these parameters from the measured characteristics, obtaining the following values:

$$g_m = 146\left.\frac{pA}{V}\right|_{\substack{V_{ds}=3.0\text{ V}\\ V_G=0.5\text{ V}}} \qquad r_o = 5.2\text{ G}\Omega\left|_{\substack{V_{ds}=3.0\text{ V}\\ V_G=0.5\text{ V}}}\right.$$

An important parameter for circuit design is the maximum voltage gain $A_{V_{max}}$ of the transistor, given by the product of the transconductance g_m and the output resistance r_o, which gives the result

$$|A_{V_{max}}| = g_m r_o = 0.76$$

Such a value represents a reasonably good result[14] when compared to other small-channel devices which normally exhibit gain in the range between 0.3 and 0.5 (see Table 1). It is important to notice that the difficulty in creating an ideal Ohmic molecule−metal contact and the resulting potential barriers at the interface determines the device performances.[8,15] Molecular engineering and the improvement of injection using different metals and/or other device geometries thus leaves many opportunities for improving the device and for achieving gain values greater than one. Another crucial issue is the self-assembly of the molecular layer, since local changes in the organization of molecules

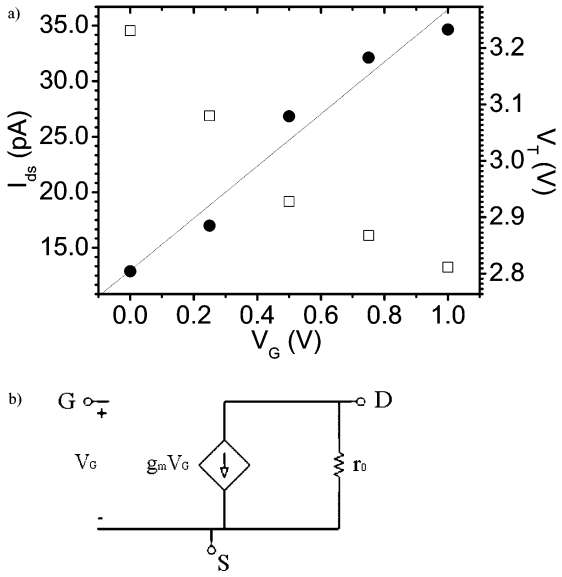


Figure 3. (a) Left scale: dependence of the drain−source current (I_{ds}, hollow squares) at $V_{ds} = 2.0$ V on the gate voltage V_G. Right scale: dependence of V_T (circles) on the gate voltage V_G. (b) Small signal equivalent circuit of a MOS transistor.

Table 1: Voltage Gain of State-of-the-Art Nanodevices and Conventional Semiconductor Transistors[a]

ref	molecule/ technology	av	
S. Tans et al. *Nature 393*, 49	CNTs	0.35	
J. Appenzeller et al. *Phys. Rev. Lett. 89*, 126801	CNTs	0.5	
this work	DNA nucleosides	0.76	
typical devices data-sheet	CMOS 0.35 μm	50	3.7
	CMOS 0.18 μm	31	10
	CMOS 0.13 μm	15	6
		weak inversion	strong inversion

[a] The active molecule or the device technology is quoted in the central column. For conventional MOSFET, gain was shown both in weak and strong inversion.

behave like defects in conventional semiconductor devices, limiting the device performance. From this point of view, an interesting strategy appears to be to exploit covalent bonding of molecules[16] in order to chemically control the self-assembly step.

We should point out that our hybrid molecular p-channel MOSFET exhibits some differences with respect to the standard silicon counterpart. In fact, despite the fact that our devices show an almost constant mobility, as expected in the standard MOS transistor model,[17] resulting in an almost linear dependence (see Figure 3a) of I_{ds} on V_G for a given V_{ds}, the expected saturation of I_{ds} does not occur.[18] This suggests a description of our devices in terms of band alignment and resonant transport in the molecular layer, where the shift of V_T is due to the modification of the molecular bands induced by the gate potential. Figure 4 sketches this mechanism: at $V_g = 0$, when V_{ds} reaches V_T (Figure 4a), resonant tunneling due to level alignment occurs. If V_g is increased by ΔV_G (Figure 4b), a shift in the molecular band is induced, resulting in a different alignment condition.

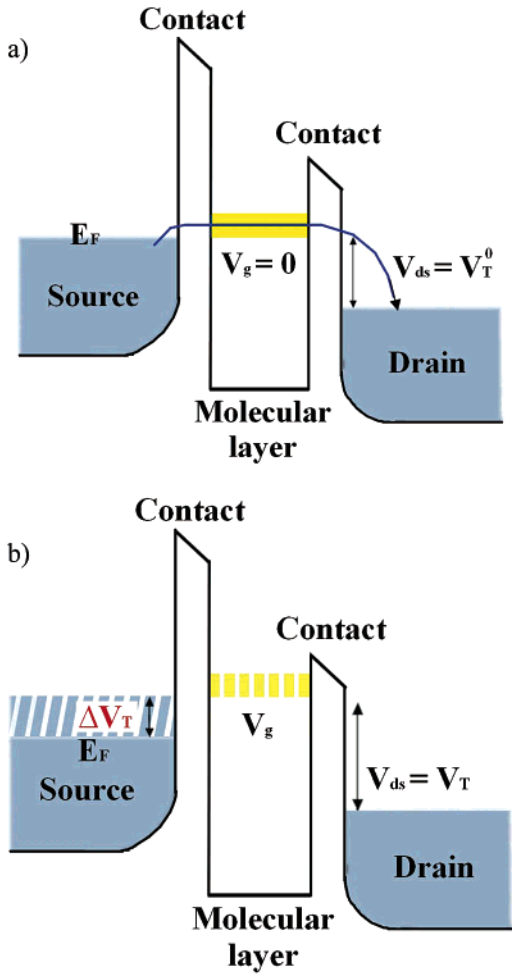


Figure 4. (a) Resonant tunneling due to level alignment at $V_{ds} = V_T^0$. The yellow bar represents the molecular electronic band at $V_G = 0$. (b) The application of a gate bias V_g induces a shift of the energy bands which results in a different alignment condition. Therefore an additional ΔV_T between source and drain has to be provided to activate the conduction process.

In this case an additional ΔV_T is needed to activate transport across the structure, consistent with the results of Figure 3a.

Finally, a few comments on device reproducibility, aging, and lifetime. From a complete statistical analysis carried out over an ensemble of 30 devices (with tip-separation of 100 nm or less), four exhibited transistor-like behavior. The others were destroyed after the first run of measurement. In most cases, upon repeating the measurements the current reduces until it vanishes after some cycles, exhibiting the well-known problem of aging.[7,19] This is primarily due to molecular layer degradation and to electrodes burning.[13] We distinguish two main problems concerning our devices. (1) The high field originating at the interface between the metallic contact and the insulator layer due to the proximity of the electrodes and their shape. The arrow-shaped electrodes clearly exhibit critical break points, strictly related to the regions where the electric field is higher (tips and constrictions). These results suggest that the shape of the nanodevices has to be carefully designed, to avoid discharging and field-induced damage.[20] In addition a careful handling of samples in order to prevent electrostatic discharge on contact is needed. (2) Differences in the layer homogeneity due to the differences in the self-assembly of molecules. This may also result in a random orientation of the guanosine dipole between the tips, with a consequent change of the built-in dipole field, resulting in different transport properties, as previously reported.[11] Due to the noncovalent bonding nature of the self-assembly (molecules are physisorbed on the substrate), a complete control of this process appears to be difficult. The need for high throughput and long-term stability thus remains a critical issue for practical applications of such hybrid devices.

In conclusion, we have fabricated a field effect transistor exploiting a modified DNA base (deoxyguanosine derivative). The interest in such molecular device derives mainly from the following features: (i) the voltage threshold for the conduction can be modulated by means of a control gate voltage V_G; (ii) the very small size of the device, and (iii) the prospect of large integration at low cost. We are working to improve both gain and on−off ratio in order to make these devices useful for logic applications. However, an on−off ratio around 5 could be enough for some logic application, such as static random access memory (S-RAM). Other molecular device prototypes have similar values.[5]

References

(1) (a) Gottarelli, G.; Masiero, S.; Mezzina, E.; Spada, G. P.; Mariani, P.; Recanatini, M. *Helv. Chim. Acta* **1998**, *81*, 2078. (b) Gottarelli, G.; Masiero, S.; Mezzina, E.; Pieraccini, S.; Rabe, J. P.; Samorì, P.; Spada, G. P. *Chem. Eur. J.* **2000**, *6*, 3242. (c) Giorgi, T.; Grepioni, F.; Manet, I.; Mariani, P.; Masiero, S.; Mezzina, E.; Pieraccini, S.; Saturni, L.; Spada, G. P.; Gottarelli, G. *Chem. Eur. J.* **2002**, *8*, 2143.

(2) Lehn, J. M.; Supramolecular Chemistry−concept and perspectives", VCH: Weinheim, 1995.

(3) Eigler, D. M.; Lutz, C. P.; Rudge, W. W. *Nature* (London) **1991**, *352*, 600.

(4) Seminario, J.; M.; Zacarias, A. G.; Tour, J. M. *J. Am. Chem. Soc.* **2000**, *122*, 3015.

(5) Reed, M. A.; Chen, J.; Rawlett, A. M.; Price, D. W.; Tour, J. M. *APL* **2001**, *78*, 3735.

(6) Aviram, A.; Ratner, M. A. *Chem. Phys. Lett.* **1974**, *29*, 277.

(7) Metzger, R. M.; Chen, B.; Hopfner, U.; Lakshmikantham, M. V.; Vuillaume, D.; Kawai, T.; Wu, X.; Tachibana, H.; Hughes, T. V.; Sakurai, H.; Baldwin, J. W.; Hosch, C.; Cava, M. P.; Brehmer, L.; Ashwell, G. J. *J. Am. Chem. Soc.* **1997**, *119*, 10455.

(8) Appenzeller, J.; Knoch, J.; Derycke, V.; Martel, R.; Wind, S.; Avouris, Ph. *Phys. Rev. Lett.* **2002**, *89*, 126801.

(9) Tans, S. J.; Verschueren, A. R. M.; Dekker, C. *Nature* **1998**, *393*, 49.

(10) Dodabalapur, A.; Katz, H. E.; Torsi, L.; Haddon, R. C. *Appl. Phys. Lett.* **1996**, *68*, 1108.

(11) Rinaldi, R.; Maruccio, G.; Biasco, A.; Arima, V.; Cingolani, R.; Giorgi, T.; Masiero, S.; Spada, G. P.; Gottarelli, G. *Nanotechnology* **2002**, *13*, 398.

(12) The orientation of the ribbons with respect to the nanotips axis is somewhat random, resulting in different degrees of rectification (asymmetry of the $I-V$ curve) in different devices. Maximum rectification is obtained when the ribbons are parallel to the tip axis, whereas no rectification is obtained in the unlikely event of ribbons perpendicular to the tip axis. In the case of the present derivative the ribbons are likely to be parallel to each other in the solid state.[1c] The probability of the ribbons being perpendicular to the tip axis is low; in most cases the ribbons are oriented at an arbitrary angle with respect to the tip axis, so that a sizable dipole-field component exists along it. This induces the rectification, with typical rectification ratio of the order of 3.

(13) Maruccio, G.; Visconti, P.; D'Amico, S.; Calogiuri, P.; D'Amone, E.; Cingolani, R.; Rinaldi, R.; *Microelectron. Eng.*; in press.

(14) An analogous behaviour is observed in the reverse region of the $I-V$ curves. Though the slopes are smaller, the dependences of both threshold voltage V_T and drain−source current (at a fixed V_{ds}) on the gate voltage V_G are still linear. A value of 0.66 is obtained for the maximum voltage gain.
(15) Malenfant, P. R. L.; Dimitrakopoulos, C. D.; Gelorme, J. D.; Kosbar, L. L.; Graham, T. O.; Curioni, A.; Andreoni, W. *Appl. Phys. Lett. 80*, 2517−2519.
(16) Cingolani, R.; Rinaldi, R.; Maruccio, G.; Biasco, A. *Physica E 13*, 1229.
(17) Street, R. A.; Knipp, D.; Volkel, A. R. *Appl. Phys. Lett.* **2002**, *80*, 1658.
(18) The lack of saturation in the drain−source current makes the output current quite sensitive to small changes in the drain−source voltage and gives rise to the issues of stability against drift. If the operation conditions are changed, a decrease of both output resistance and gain can be generated.
(19) Park, J.; Pasupathy, A. N.; Goldsmith, J. I.; Chang, C.; Yaish, Y.; Pette, J. R.; Rinkoski, M.; Sethna, J. P.; Abruna, H. D.; McEuen, P. L.; Ralph, D. C. *Nature* (London) **2002**, *417*, 722.
(20) Free-standing electrodes separated by few nanometers were used in the past to measure conductivity in organic and biological molecules.[21,22] Moreover, this particular geometry is not suitable in our case, since the used cast deposition method for the self-assembly requires a surface to take place.
(21) Porath, D.; Bezryadin, A.; de Vries, S.; Dekker, C. *Nature* (London) **2000**, *403*, 635.
(22) Di Fabrizio, E.; Grella, L.; Baciocchi, M.; Gentili, M.; Ascoli, C.; Cappella, B.; Frediani, C.; Morales, P. J. *Vac. Sci. Technol. B 15*, 2892.

NL034046C